Journal of Nuclear Materials 394 (2009) 87–94

Contents lists available at ScienceDirect

Journal of Nuclear Materials

journal homepage: www.elsevier.com/locate/jnucmat

Microstructural analysis of MTR fuel plates damaged by a coolant flow blockage

A. Leenaers *, F. Joppen, S. Van den Berghe

SCK•CEN, Nuclear Materials Science Institute, Boeretang 200, B-2400 Mol, Belgium

ARTICLE INFO

Article history:
Received 17 April 2009
Accepted 11 August 2009

ABSTRACT

In 1975, as a result of a blockage of the coolant inlet flow, two plates of a fuel element of the BR2 reactor of the Belgian Nuclear Research Centre (SCK•CEN) were partially melted. The fuel element consisted of Al-clad plates with 90% ^{235}U enriched UAl_x fuel dispersed in an Al matrix. The element had accumulated a burn up of 21% ^{235}U before it was removed from the reactor. Recently, the damaged fuel plates were sent to the hot laboratory for detailed PIE.

Microstructural changes and associated temperature markers were used to identify several stages in the progression to fuel melting. It was found that the temperature in the center of the fuel plate had increased above 900–950 °C before the reactor was scrammed. In view of the limited availability of such datasets, the results of this microstructural analysis provide valuable input in the analysis of accident scenarios for research reactors.

1. Introduction

Understanding the behavior of fuel elements under abnormal condition is an essential topic in the development of accident scenarios for research reactors [1–4]. For nuclear power plants the behavior of fuel under accidental conditions is well studied in international projects such as PHEBUS and VERCORS [5–7]. In contrast, similar knowledge on the behavior of the fuel under severe transient or accident conditions needed for defining accident scenarios for research reactors is rather scarce [8–11]. The information for power plants is of limited application to research reactors due to the differences in fuel type, power level and thermo-hydraulic conditions. Most research reactors operate at lower cooling water temperature and pressure, but the power density and coolant flow rates are high compared to power plants. This complicates the thermo-hydraulic analysis in transient conditions, after an initiating event.

Reactivity effects are also different. Most of the research reactors with a higher power level are loaded with fuel to maintain significant excess reactivity (several times prompt criticality), which can give more severe reactivity transients. On the other hand, the fuel surface-to-volume ratio is much greater for plate type fuel than for pin type fuel. This leads to more local boiling during overheating of the fuel plate and more negative temperature coefficients.

A credible accident scenario with relatively high probability is a fuel channel blockage [12]. Such a partial blockage of a fuel channel occurred in the BR2 reactor of SCK•CEN in 1975. A foreign object partially blocked the entrance of a fuel element, causing an important reduction of coolant flow, resulting in the partial melting of 2 plates of the element. This incident was included in the 1985 periodic safety analysis of BR2 and in the IAEA database (Incident Reporting System Research Reactors).

2. Local flow blockage incident

In 1975, an 8-sector element was irradiated in a 200 mm channel of the BR2 reactor at SCK•CEN. The fuel sector (ATR type) was made up of 13 rolled, curved plates, which were mechanically fixed by the roll swaging technique into solid grooved radial stiffeners. The Al-clad fuel plates consisted of highly enriched uranium aluminide (90% ^{235}U) dispersed in an aluminum matrix.

A few hours after the start of the reactor, an automatic stop occurred due to high activity of the primary water. The power of the reactor at that moment was 48.3 MW (60% of the reference power of that cycle). Analysis of the activity of the primary water indicated immediately that a significant part of the surface of a fuel element must have been damaged. It was estimated that between 40 and 120 cm^2 of the plate surface had melted and that the quantity of uranium lost in the primary circuit was about 6 g. Unloading of the core showed that the entrance of fuel element A030 was blocked by a foreign object, which was later on identified as the plastic handle of a screwdriver that had dropped in the fuel channel during loading [13].

The initial signal to stop the reactor came from the high pressure ionizing chambers mounted on the exit of the primary pipe. These chambers are used to measure ^{16}N activity in the primary circuit in order to have a direct indication of the power of the reactor. It is interesting to note that these chambers reacted several

* Corresponding author. Tel.: +32 14 333044; fax: +32 14 321216.
E-mail address: aleenaer@sckcen.be (A. Leenaers).

0022-3115/$ - see front matter © 2009 Elsevier B.V. All rights reserved.
doi:10.1016/j.jnucmat.2009.08.014

minutes before those that are designed to detect the released fission products. This is due to their close location to the reactor core and their high sensitivity for γ-radiation.

In the minutes following the incident, the activity of ^{88}Kr in the primary circuit was measured on-line to be about 100 GBq/m^3 giving a total quantity in the primary circuit of 15 TBq. Concentration of ^{131}I was measured to be 3.7 GBq/m^3 or a total quantity of 550 GBq. Since BR2 has a closed loop, pressurized primary circuit, this activity remained mainly in the primary circuit and was removed by purification with ion exchange resins, degassing and natural decay. The main inconvenience was that a number of locations were temporarily inaccessible. After the incident, the purification with ion exchangers was set to maximum capacity (40 m^3/h for a volume of 150 m^3). The concentration of ^{88}Kr subsequently decreased to 40 MBq/m^3 and the iodine from 131 to 22 MBq/m3. At that moment, the reactor could be opened and the fuel unloaded, including the damaged fuel element. The reactor was restarted two weeks after the incident.

Recently, the defective fuel element was dismantled and, in view of the scarcity of data on research reactor fuel behavior under accidental conditions, the damaged fuel plates were sent to the Laboratory for High and Medium Activity (LHMA) at the SCK•CEN site for microstructural examination.

3. Microstructural examination

The Al1100 clad fuel plates consisted of high enriched uranium aluminide (90% ^{235}U) dispersed in an aluminum matrix. The uranium aluminide was fabricated from a melting and casting operation and as a result usually contained a mixture of UAl_3, UAl_4 and UAl_2. A typical composition is around 63% UAl_3, 31% UAl_4 and 6% UAl_2 [14]. Such a composition is referred to as UAl_x. As UAl_2 is fairly reactive, it reacts with the excess aluminum during rolling of the plates, to form UAl_3 and UAl_4. Although there exists some uncertainty in the compositional phase boundaries of the UAl_4 phase [15], it is known to exist [16,17]. One can therefore assume that the finished fuel plates contained only UAl_3 and UAl_4.

The sector assembly involved in the incident was used for three irradiation cycles of 20.8, 7.4 and 19.6 operating days respectively before the incident happened. At the EOL of the sector, the average burn up was calculated to be 21% ^{235}U.

Visual inspection in the hot cell showed that for one of the plates (Fig. 1) almost 50% of the meat zone has melted. In the center of this zone, part of the fuel plate is missing. Most of this material would have been released in the primary circuit but part of it might have been pulled out during transport and handling of the plates.

A more detailed image (Fig. 2) of the least damaged fuel plate shows that the affected region consists of 3 areas with different structural aspects:

- the intact cladding;
- an area showing a rough surface structure that might be the result of oxide flakes that peeled off;
- a very dark colored area and at some positions material is missing.

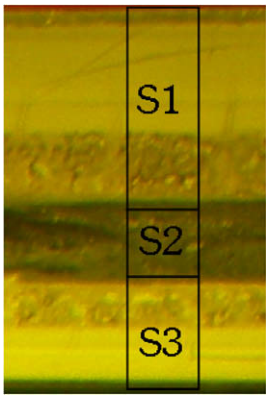

Fig. 2. Optical image of part of the fuel plate.

A slice was cut from the least damaged fuel plate (Fig. 1) and subdivided in three samples (S1, S2, S3) (Fig. 2). The samples were embedded in such a way that the complete section of the fuel (meat and cladding) could be observed.

In the backscattered electron image of the cross section of sample S1, shown in Fig. 3, different zones can be identified. The fuel and the cladding in zone A appear to be unaffected by the incident and can be considered to represent the intact fuel plate.

In zone B, one observes a transition in the meat from dense to porous fuel particles. The cladding is still intact but a slight increase in the plate thickness is observed. In zone C, large pores appear in the meat, and in the cladding precipitation is seen at the grain boundaries. In this region, the swelling in the fuel plate has increased even further. In zone D, the meat and the cladding can no longer be distinguished. The severe contraction in the plate thickness and the cracking throughout the cladding indicate that all fission gas was released at this position and the fuel plate was reduced to a melt.

The microstructure of sample S2 (middle of the fuel plate) is that of a resolidified material. In sample S3, similar zones as in sample S1 could be observed. The different stages before melting of the fuel plate can thus be identified. A more detailed microstructural analysis of each zone was performed to determine the associated temperatures.

3.1. Sample S1

The collage of backscattered electron images (BEI) in Fig. 4a covers the complete plate cross section in zone A. A thick (~15 μm) oxide layer on the outer surface (Fig. 4b) of the cladding can be observed. This oxide layer has cracked both perpendicular and parallel to the surface. The cracks parallel to the surface could indicate that the oxide consists of multiple layers, possibly related to the different reactor cycles. The perpendicular cracks usually result from dehydration of the layer during the drying of the fuel plate in the hot cell [18].

The meat consists of ground fuel particles dispersed in an Al matrix. Most of the UAl_x particles show cracks, demonstrating

Fig. 1. Pictures of the two damaged fuel plates.

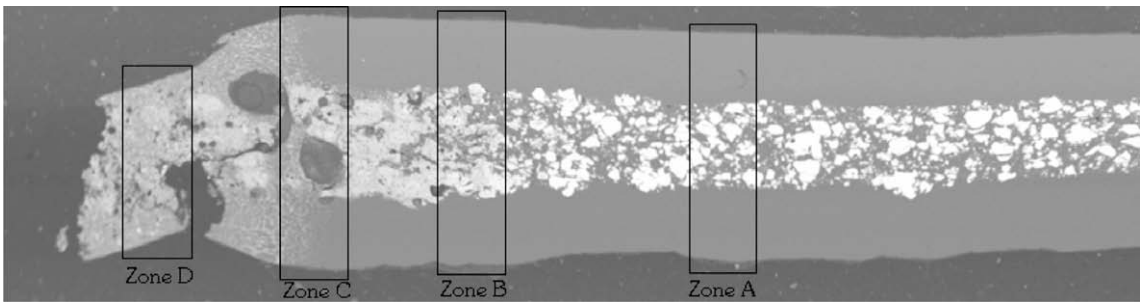

Fig. 3. The backscattered electron image covering the cross section of sample S1.

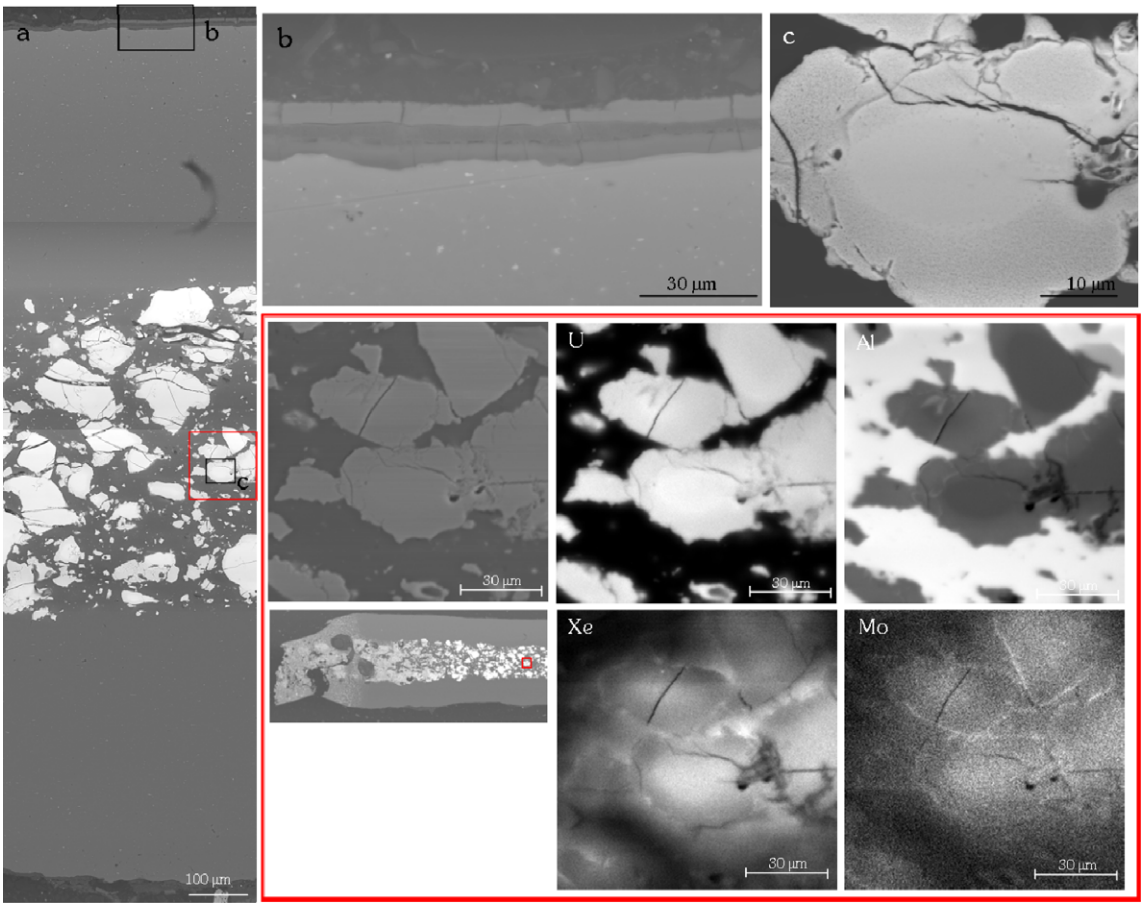

Fig. 4. BEI image across the plate section at zone A (a) and detailed BEI image of the oxide layer (b) and a fuel particle (c). The EPMA X-ray maps are contained within the red frame. (For interpretation of the references to color in this figure legend, the reader is referred to the web version of this article.)

the brittle nature of the fuel. In a more detailed image of a fuel kernel (Fig. 4c), one can observe a layer around the particle, which contains a lot of small bubbles. From the electron microprobe analysis (EPMA), (Fig. 4 within the red frame) it is seen from the X-ray mapping of U and Al that this layer is richer in Al than the particle interior. Local quantitative analysis (Table 1) confirms that it is a $U_{0.9}Al_4$ layer while the fuel particle is UAl_3–UAl_4. The $U_{0.9}Al_4$ layer is the result of the interaction between the UAl_x and Al matrix. These interaction layers are also found in other types of dispersion fuels. In several studies, this interaction layer is, regardless of the composition of the plate type fuel, characterized as amorphous [19]. This was directly demonstrated for U(Mo) dispersion fuel in [20]. The amorphous nature of these interaction layers is explained as the result of their formation mechanism, which is related to the mixing of fuel material with the matrix by the fission product tracks. One can assume that the $U_{0.9}Al_4$ layer found in this study also is amorphous, but currently no experimental data is available to confirm this. The presumed amorphous nature of the interaction layer would explain why the fission gas bubbles are observed only

Table 1
Quantitative results from EPMA analysis performed in the different zones.

		Wt% Al	Wt% U	Phase
Zone A	Intact fuel kernel	25.5	68.5	UAl_3–UAl_4
	Interaction layer	33.0	63.0	$U_{0.9}Al_4$
Zone B	Fuel particle	36.2	68.8	$U_{0.9}Al_4$
Zone C	Small particles	33.5	67.0	$U_{0.9}Al_4$
Zone D	Angular particles	25.0	69.8	UAl_3
	Rounder particles	34.9	68.0	$U_{0.9}Al_4$

in the interaction layer. In the fuel particle interior, the fission gas is probably still contained within nanobubbles [20].

The fission gas retention is also confirmed by the EPMA results. The Xe and Mo X-ray maps all show the presence of all fission products inside the fuel kernel. In the interaction layer, a lower concentration of fission products is measured. For Xe, this is at least partially related to the sample preparation (the bubbles get opened during polishing). Around the fuel particle, on the interface with the matrix, the typical fission product halo can be seen.

In zone B, we can still distinguish the meat from the cladding (Fig. 5a). Most of the oxide layer on the outer surface of the cladding is spalling off, but a small layer is still attached to the cladding (Fig. 5b).

Inside the meat, a transition in the morphology of the fuel particles is observed. At the right side of Fig. 5a, intact fuel particles are seen, while to the left, the fuel starts to contain large bubbles or pores and the particles become larger and more rounded.

In a more detailed image (Fig. 5c), it is seen that the interiors of the intact particles contain many small (100–300 nm) bubbles. In the interaction layer, the size of the fission gas bubbles has increased, by coalescence with neighboring bubbles. This onset of fission gas release causes the fuel particles to swell and assume a more rounded appearance. Consequently, the plate thickness in Zone B increases (Fig. 3). The solid state reaction rate between the fuel kernel and the aluminum matrix accelerates and consumes the entire kernel.

This is confirmed in the EPMA X-ray maps. In the right part of the Xe X-ray map, fission gas is still measured in the particles while at the left side almost none is detected. The Al and U maps show that the fuel particles at the left side are richer in Al, indicating a complete interaction of the particles with the Al matrix, forming $U_{0.9}Al_4$ (Table 1).

In zone C, the meat can still be distinguished from the cladding (Fig. 6a). Fig. 6b and the O X-ray map (EPMA, top row) clearly show

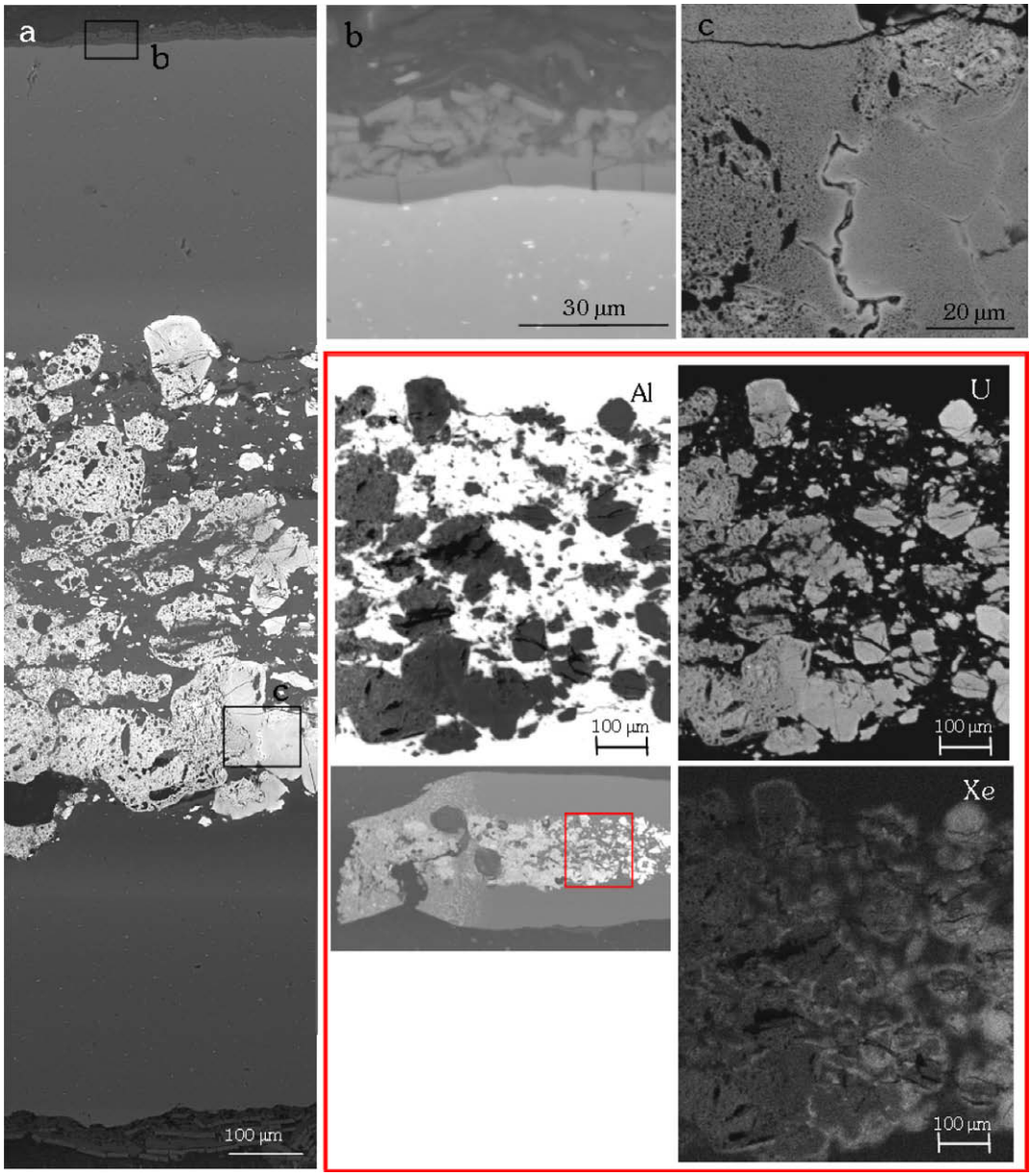

Fig. 5. BEI image across the plate section at zone B (a) and detailed BEI image of the oxide layer (b) and a fuel particle (c). The EPMA X-ray maps are contained within the red frame. (For interpretation of the references to color in this figure legend, the reader is referred to the web version of this article.)

the presence of an oxide layer (thickness 5 μm) on the outer surface of the cladding.

In the cladding, a different phase is present at the grain boundaries (Fig. 6b). From the EPMA Al and U maps (top row), it is seen that this feature is associated with uranium aluminide, which has diffused into the cladding via the grain boundaries.

In the meat, it is no longer possible to differentiate the fuel particles from the matrix. Also here, uranium is present on the Al grain boundaries (Fig. 6c and EPMA bottom row), while the observed particles can be identified as $U_{0.9}Al_4$.

Further fission gas bubble coalescence has occurred resulting in very large round pores seen in the former meat region of the plate. The swelling of the meat resulting from this is also reflected in the thickness of the fuel plate at this position (Fig. 3).

In zone D (Fig. 7a), no clear difference can be made between the meat and the cladding. Pure Al grains are observed, and on the grain boundary the uranium aluminide phase formed a eutectic microstructure. The $U_{0.9}Al_4$ particles can be found at several places but they seem more concentrated in the center of the plate (Fig. 7a and c).

The EPMA measurements confirm these findings. They also show the presence of an approximately 5 μm thick oxide layer remaining on the outer surface (EPMA results, top row and Fig. 7b). This layer contains cracks perpendicular to the surface, indicating dehydration of the oxide sheet. Note that no uranium is measured within this oxide layer, indicating that the layer was formed prior to the incident.

Some smaller rounded pores, related to the fission gas release can still be seen but the thickness of the plate in this zone is severely reduced. Large cracks running through the meat and cladding (Figs. 3 and 7a) also indicate that the complete fission gas inventory has been released, leaving behind a pool of molten aluminum with small $U_{0.9}Al_4$ particles in it.

It is observed that the inner surface of the large cracks are covered with an oxide layer. In this oxide layer, aluminum and uranium can be measured, indicating that the layer was formed during or after the incident.

3.2. Sample S2

The microstructure of the resolidified material in sample S2 (Fig. 8a) looks nearly identical to zone D in sample S1. However, from more detailed BEI images (Fig. 8b) it is observed that large angular particles have formed, which can be identified as UAl_3 (Table 1). The smaller, rounder particles (denoted by red circles in Fig. 8b) are the previously observed $U_{0.9}Al_4$ particles (Table 1). More to the right in Fig. 8a (more to the center of the fuel plate), the formation of some dendrites is observed (Fig. 8c). In the area covered by Fig. 8d, almost solely dendrites are observed in the melt. These dendrites shown in Fig. 8d consist of UAl_3, while the small particles at the extremities of the branches contain only a few wt% U.

4. Discussion

According to literature on these types of incidents, a first rapid release of fission gas will occur at temperatures around the blistering temperature. The release will increase upon reaching the solidus temperature of the cladding and at the U–Al eutectic temperature [21–24]. For the fuel plates under consideration this would be respectively, 565 °C (blistering temperature), about

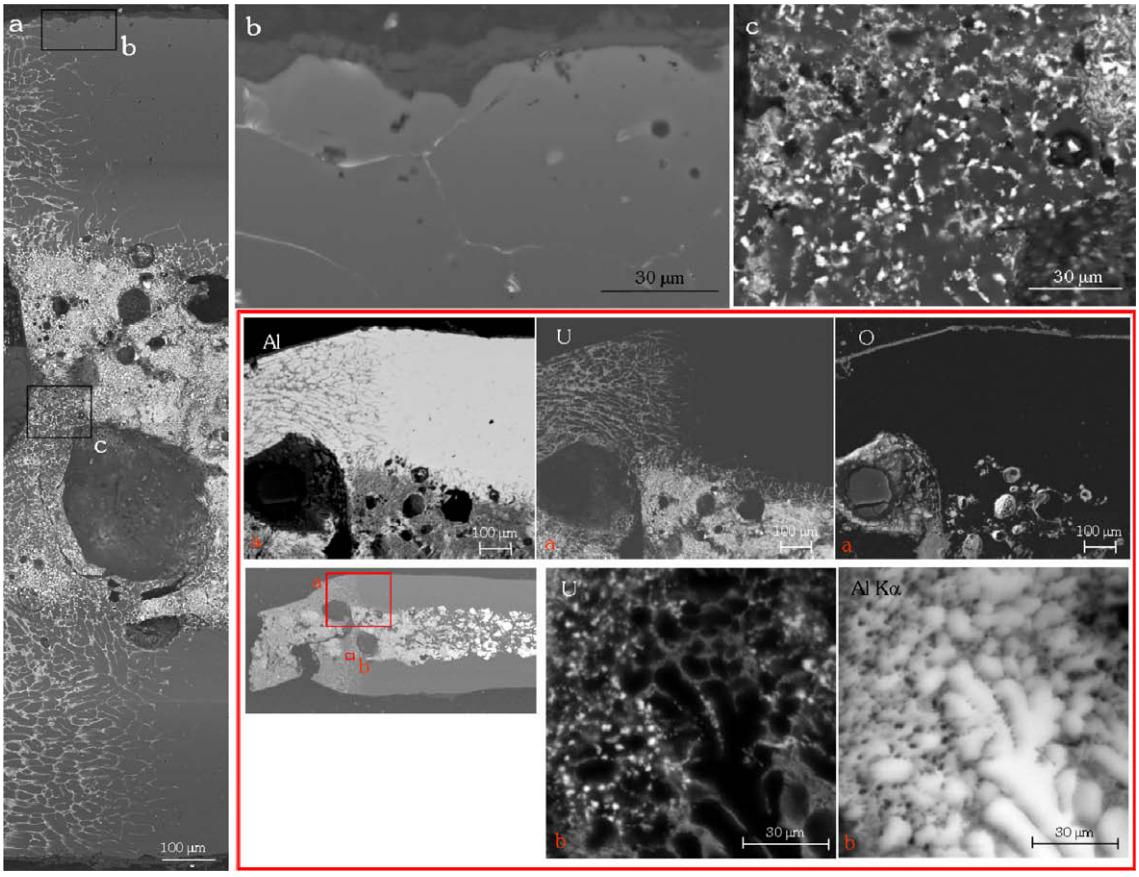

Fig. 6. BEI image across the plate section at zone C (a) and detailed BEI image of the oxide layer (b) and a fuel particle (c). The EPMA X-ray maps are contained within the red frame. (For interpretation of the references to color in this figure legend, the reader is referred to the web version of this article.)

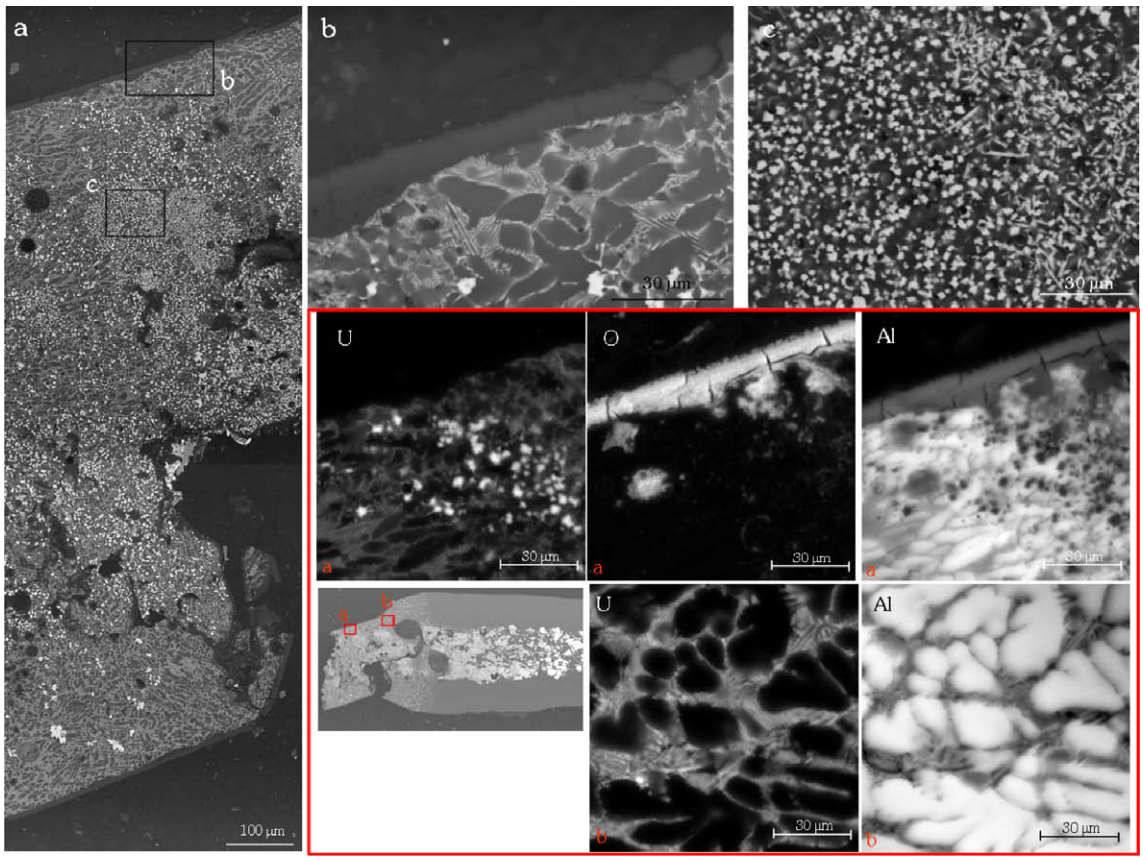

Fig. 7. BEI image across the plate section at zone D (a) and detailed BEI image of the oxide layer (b) and a fuel particle (c). The EPMA X-ray maps are contained within the red frame. (For interpretation of the references to color in this figure legend, the reader is referred to the web version of this article.)

646 °C (solidus temperature for an 1100 grade cladding) and 641 °C (U–Al eutectic).

Based on this information, the observed microstructure and the binary diagram (Fig. 9), it is possible to indicate the local temperatures in the different zones and samples.

In zone A, the fuel plate shows microstructural features typical for fuel operated under normal conditions, that is, the temperature of the fuel would have reached around 200 °C if the reactor was at full power. Even at this low temperature a solid state reaction between the UAl_3 fuel and the Al matrix takes places, resulting in the formation of an $U_{0.9}Al_4$ interaction layer. This layer shows behavior similar to that noted in other amorphous reaction products in allowing the growth of larger fission gas bubbles. The remaining fission gas is expected to be contained in nanobubbles lying in the UAl_3 kernel. The zone A thus corresponds to the intact fuel plate, in Fig. 2.

The subsequent zone B, C and D are transition zones in which the microstructure evolves over a very narrow width. In zone B, a clear onset for fission gas release is observed. This means that the fuel temperature was probably increasing to 550 °C. According to literature, fission gas release below 550° is negligible [21], but it does cause the fuel plate to swell.

The higher temperature has also accelerated the solid state reaction between the UAl_3 fuel particles and the Al matrix, as all the fuel is transformed into $U_{0.9}Al_4$ particles.

The totally fractured outer oxide layer observed in zone B could be consistent with the observations on the area in Fig. 2 where the oxide flakes appear to have spalled off from the cladding surface.

The appearance of uranium aluminide on the Al grain boundaries in zone C indicates that incipient melting at the Al grain boundaries is likely to have occurred, giving easy access pathways for the uranium to diffuse. This means that the temperature in this zone must have been close to 646 °C, the solidus temperature of the cladding.

Not only would the molten Al grain boundaries have been easy access paths for diffusion of the fuel but also fission gas will have been transported out of the fuel and through the cladding. This is consistent with the first fission gas release at the cladding solidus temperature as reported in literature.

Increasing fission gas bubble coalescence and mobility results in the formation of larger fission gas bubbles, which in turn cause a substantial increase in plate thickness (Fig. 3).

The transition from Zone C to D is characterized by necking of the fuel plate (Fig. 3). In Zone D, the plate thickness has substantially decreased and large cracks are running through the meat and cladding. No more large fission gas pores are seen as a full release of the fission gas inventory has occurred. The observation of a eutectic microstructure at the cladding grain boundaries points out that the temperature went beyond 660 °C, but, since in the former meat section only $U_{0.9}Al_4$ precipitates are measured, we should conclude, based on the binary diagram, that the temperature in this zone stayed below 731 °C.

The fuel plate at this location is thus reduced to a melt in which the reaction between the remaining solid cladding material and the fuel is nearing completion. Zone D therefore shows the transition from a partially solid to a fully molten structure as observed in sample S2 and corresponds to the start of the dark colored area in Fig. 2. The surface in zone D is still covered by a thin oxide layer.

Local quantitative analysis shows and reference to literature [25], shows that in the area of sample S2 beyond zone D of S1, large angular UAl_3 particles are found in addition to the $U_{0.9}Al_4$ particles.

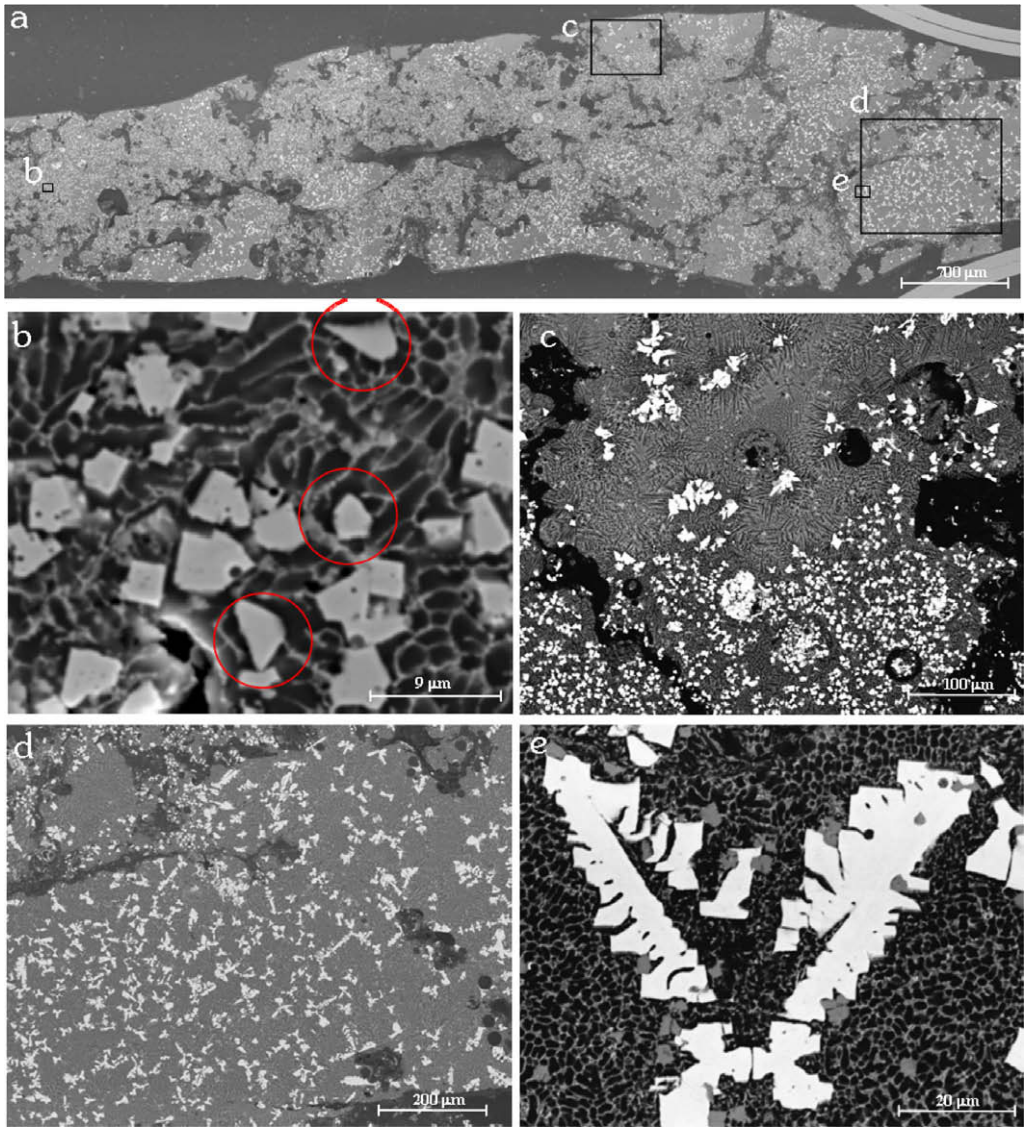

Fig. 8. BEI images covering sample S2 (a). More detailed images reveal the microstructures observed (b–e).

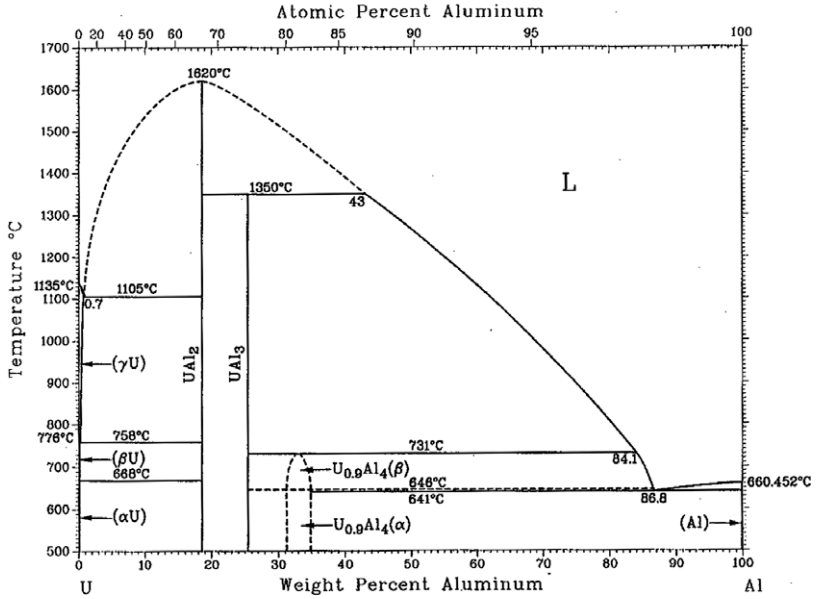

Fig. 9. Binary U–Al diagram [16].

More towards the center of the fuel plate, UAl_3 dendrites are seen. At the extremities of these dendrites, eutectic droplets are observed (gray particles in Fig. 8e). These observations and the assumption that the average composition of the melt is around 72–75 wt% Al (supported by EDX and image analysis), indicate from the binary diagram (Fig. 9) that the temperature in this location must have reached at least 900–950 °C.

Even though the temperature was high enough to melt the fuel and the pure Al cladding, it was not high enough to melt the aluminum oxide layer on the outer surface of the cladding (melting temperature of Al_2O_3 is 2054 °C). From the observations made it is clearly seen that most of the oxide layer that has formed prior to the incident, stayed intact and, more importantly, protected the pure Al cladding from reacting with the water or steam. However, as observed in zone D, the full fission gas release will cause breaking of the cladding and as such expose pure aluminum particles to a water or steam environment. For an Al particle coming in contact with water or steam at temperatures below 1500 °C, a protective oxide layer quickly shields the particle surface and reduces the subsequent rate of oxygen uptake to essentially zero [26]. The growth of such a protective oxide layer during the incident, is observed on the inner surface on the cracks in the cladding resulting from the fission gas release.

5. Conclusion

The behavior of fuel elements under abnormal conditions is important tot the analysis of accident scenarios of research reactors. The incident that occurred at the BR2 reactor in 1975 presents a case study of fuel plate damage due to coolant flow blockage.

The local coolant flow blockage caused the partial melting of two fuel plates. Detailed analysis shows that the microstructure of the melted plate is defined by full fission gas release, the complete reaction between UAl_x fuel and the Al matrix and weakening of the cladding. All phenomena were driven by the increasing temperature, which has probably reached >900 °C in the center of the fuel plate, before the reactor scrammed.

The behavior of fission gas release and the thermodynamic evolution of the phases have been clearly identified through microstructural analyses.

Acknowledgement

The authors are indebted to Dr. A. De Bremaecker for the fruitful discussions and to our colleague D. Sears from AECL (Atomic Energy Canada Limited) for his valuable input.

References

[1] Q. Lu, S. Qiu, G.H. Su, Nucl. Eng. Des. 239 (2009) 45.
[2] M. Adorni, A. Bousbia-Salah, T. Hamidouche, B. Di Maro, F. Pierro, F. D'Auria, Ann. Nucl. Energy 32 (2005) 1679.
[3] M. Adorni, A. Bousbia-Salah, F. D'Auria, T. Hamidouche, The Proceedings of the International Conference Nuclear Energy for New Europe, Portoroz, Slovenia, 2007.
[4] J.E. Matos, in: The Proceedings of the US/IAEA Regional Workshop on Application of the Code of Conduct on the Safety of Research Reactors, Argonne National Laboratory, 2007.
[5] G. Ducros, P.P. Malgouyres, M. Kissane, D. Bouland, M. Durin, Nucl. Eng. Des. 208 (2001) 191.
[6] P. Von der Hardt, A.V. Jones, C. Lecomte, A. Tattegrain, Nucl. Saf. 35 (2) (1994).
[7] B.J. Lewis, R. Dickson, F.C. Iglesias, G. Ducros, T. Kudo, J. Nucl. Mater. 380 (2008) 126.
[8] P.G. Ellison, P.R. Monson, M.L. Hyder, in: The Proceedings of the 27th ASME/AICHE/ANS National Heat Transfer Conference, Minneapolis, US, 1991.
[9] J.H. Buddery, K.T. Scott, J. Nucl. Mater. 5 (1961) 81.
[10] K. Yanagisawa, T. Fujishiro, O. Horikj, K. Soyama, H. Ichikwa, T. Kodaira, J. Nucl. Sci. Technol. 29 (1992) 233.
[11] Z.T. Mendoza, C.A. Stevens, R.L. Ritzman, Nucl. Technol. 53 (1981) 155.
[12] IAEA, Safety Reports Series No. 53, 2008.
[13] F. Joppen in: The Proceedings of the 9th International Topical Meeting on Research Reactor Fuel Management (RRFM), Budapest, Hungary, 2005.
[14] D. Stahl, ANL-83-5, 1982.
[15] M.E. Kassner, P.H. Adler, M.G. Adamson, D.E. Peterson, J. Nucl. Mater. 167 (1989) 160.
[16] O. Tougait, H. Noel, Intermetallics 12 (2004) 219.
[17] A.E. Dwight, Argonne National Laboratory Report No. ANL-82-14, Argonne, IL, 1982.
[18] A. Leenaers, E. Koonen, Y. Parthoens, P. Lemoine, S. Van den Berghe, J. Nucl. Mater. 375 (2008) 243.
[19] J. Rest, in: The Proceedings of the 23rd International Meeting on Reduced Enrichment for Research and Test Reactors (RERTR), Las Vegas, Nevada, USA, 2000.
[20] S. Van den Berghe, W. Van Renterghem, A. Leenaers, J. Nucl. Mater. 375 (2008) 340.
[21] T. Shibata, K. Kanda, K. Mishima, T. Tamai, M. Hayashi, J. L. Snelgrove, D. Stahl, J.E. Matos, F.N. Case, J.C. Posey, in: The Proceedings of the International Meeting on Research and Test Reactor Core Conversions from HEU to LEU Fuels, ANL, 1982.
[22] NUREG-1313, 1988.
[23] J.M. Beeston, R.R. Hobbins, G.W. Gibson, W.C. Francis, Nucl. Technol. 49 (1980) 136.
[24] R.P. Taleyarkhan, Nucl. Saf. 33 (1) (1992).
[25] V.Y. Zenou, G. Kimmel, C. Cotler, M. Aizenshtein, J Alloys Compd. 329 (2001).
[26] M. Epstein, H.K. Fuaske, T.G. Theofanous, Nucl. Eng. Des. 201 (2000) 71.